Scientific Contributions Oil & Gas, Vol. 48. No. 1, April: 43 - 62

SCIENTIFIC CONTRIBUTIONS OIL AND GAS
Testing Center for Oil and Gas
LEMIGAS

Journal Homepage:http://www.journal.lemigas.esdm.go.id
ISSN: 2089-3361, e-ISSN: 2541-0520

Stress Regime Analysis in The Structural Transition Between Sumatra and Jawa

Hikhmadhan Gultaf[1], Benyamin Sapiie[1], Wahyu Triyoso[2], Meli Hadiana[1], Yehezkiel Halauwet[3] and Herlina Almanda Anna Maria Narwadan[3].

[1]Department of Geological Engineering, Bandung Institute of Technology
Ganesha Street No.10, Lebak Siliwangi, Coblong, Bandung City, West Java 40132, Indonesia.

[2]Department of Geophysical Engineering, Bandung Institute of Technology
Ganesha Street No.10, Lebak Siliwangi, Coblong, Bandung City, West Java 40132, Indonesia.

[3]Agency for Meteorology Climatology and Geophysics (BMKG)
Ambon, 97122, Indonesia.

Corresponding author: hgultaf@gmail.com

Manuscript received: December 16th, 2024; Revised: January 06th, 2025
Approved: January 21th, 2025; Available online: April 07th, 2025.

ABSTRACT - The structural transition between Sumatra and Java presents significant geological challenges due to the change in the orientation of the convergent plate boundary, shifting from NW-SE in western Sumatra to W-E in southern Java. This study focuses on the regions of Lampung (representing Sumatra's tectonics), West Java (representing Java's tectonics), and the Sunda Strait as the boundary between them. The research aims to map tectonic stress conditions using formal stress inversion methods based on earthquake focal mechanism data, constrained to depth intervals of 0-15 km and 15-33 km. Focal mechanism data are categorized by geographic and regional structural geology with kinematic homogeneity, leading to the identification of ten inversion zones. Findings show that Lampung's average stress regime ($\bar{R}'$) is strike-slip fault regime at both depth intervals. The Sunda Strait displays a transtensive fault regime across these depths, while West Java has a thrust fault regime at 0-15 km, transitioning to strike-slip fault regime at 15-33 km.

Keywords: stress inversion, focal mechanism, stress regime, Sunda Strait, structural transition.

How to cite this article:

Hikhmadhan Gultaf, Benyamin Sapiie, Wahyu Triyoso, Meli Hadiana, Yehezkiel Halauwet and Herlina Almanda Anna Maria Narwadan, 2025, Stress Regime Analysis in The Structural Transition Between Sumatra and Jawa, Scientific Contributions Oil and Gas, 48 (1) pp. 43-62. DOI.org/10.29017/scog.v48i1.1687.

INTRODUCTION

The Sunda Strait is in western Indonesia, within the structural transition region. The Sunda Strait separates two distinct geodynamic settings (Ghose et al. 1990) as transition zone (Budiarto 1976; Zen & Sudrajat 1983), lithosphere transition (Hamilton 1988), and boundary zone (Ranneft 1979; Huchon & Pichon 1984). To the northwest of the Sunda Strait, the N140°E-trending Sumatra Island is subducted by the Indo-Australian Plate, with an NNE vector toward Sumatra (Sieh & Natawidjaja 2000; Carton

et al. 2014; Dokht et al. 2018) about 20o-25o. To the east of the Sunda Strait, Java Island, with an axis of N100oE, is orthogonally subducted by the Indo-Australian Plate, which moves towards N3o-11oE. There is a bending of the plate boundary from Sumatra to Java. The differing tectonic conditions in Sumatra and Java result in distinct deformation patterns. Deformation in Sumatra involves simple shear, resulting primarily in strike-slip faults or faults with a dominant strike-slip component. In Java, deformation is characterized by pure shear, mainly leading to strike-slip faults or faults with a more prominent reverse dip-slip component. The impact of the subduction of the Indo-Australian Plate south of Sumatra and Java produces different stress patterns in each region, especially focused in Lampung, Sunda Strait, and West Java. This study aims to map the stress regime in the structural transition region and its implications for geomechanical fracture as a hydrocarbons pathway.

METHODOLOGY

This study primarily utilizes earthquake focal mechanism data, which are grouped into ten zones, one of which is based on a regional geological structure map developed as the basis for zone delineation. The focal mechanism data in each zone are analyzed using formal stress inversion methods to determine the principal stress axes, stress ratio R, and stress regime R', as well as maximum (SH_{max}) and minimum (Sh_{min}) horizontal stresses. The results are then used to map and interpret the stress patterns in the study area.

Data compilation

Using earthquake focal mechanism data to perform formal stress inversion provides a powerful approach to understanding stress patterns in this structural transition zone. This method can identify the stress patterns that occur due to the bending of the subduction zone in the structural transition region. This paper compiles data on earthquake focal mechanisms from various sources and categorizes them into ten zones. The earthquake focal mechanism data used are sourced from the Global CMT (The Global Centroid Moment Tensor), BMKG (Meteorology, Climatology, and Geophysical Agency), GFZ Potsdam (Geo Forschungs Zentrum), and the results of optimum inversion analysis for small-medium magnitude moments (Mw ≤ 5) using the method developed by Halauwet (Halauwet et al., 2024). The earthquake focal mechanism data also uses earthquake data with small magnitude moments. The data is divided into two depth intervals: 0-15 km, which is as much as 269 data, and 15-33 km, which is as much as 169 data (Figure 2).

Formal stress inversion method

The data for this formal stress inversion analysis is earthquake focal mechanisms to analyze the ongoing stress regime R′ in the structural transition zone of Lampung – Sunda Strait – West Java, which was analyzed using stress inversion software (e.g., Delvaux & Sperner 2003). Due to the complexity of geological conditions and processes, certain assumptions must be made when performing stress inversion. In the purpose of addressing these complexities, the following assumptions were utilized in the stress inversion process (Delvaux & Barth 2010): (1) the rocks are considered isotropic, (2) stress distribution is assumed to be consistent and constant across both space and time and (3) during an earthquake, slip movement occurs in the direction of maximum shear stress (Wallace-Bott hypothesis, Bott 1959).

Formal stress inversion entails two iterative analysis steps: improved right dihedron and rotational optimization (Delvaux & Sperner 2003). These methods aim to determine four reduced stress tensor parameters that model optimal stress conditions in a specific area. These parameters include the three principal stress axes ($\sigma_1 > \sigma_2 > \sigma_3$) and the stress ratio R, which represents the relative magnitudes of σ_1 and σ_3.

$$R = \sigma_2 - \sigma_3 / \sigma_1 - \sigma_3 \quad (1)$$

In addition to these four parameters, stress regimes R', maximum horizontal stress (SH_{max}), and Sh_{min} were also generated. Notably, SH_{max} and Sh_{min} are perpendicular to one another. The calculations for SH_{max} and Sh_{min} were interpreted using the methods outlined by Lund and Townend (Lund & Townend 2007), with the SH_{max} calculation specifically applied through the formal inversion stress program using their algorithm.

Table 1
The naming and color scale of the stress regime ware compiled from (Delvaux et al. 1997; Delvaux & Sperner 2003; Delvaux & Barth 2010).

R	0	0.25	0,5	0.75	1	0.75	0,5	0.25	0	0.25	0,5	0.75	1
Determination of R'			***R' = R***				***R' = 2 - R***				***R' = 2 + R***		
R'	0	0.25	0,5	0.75	1	1.25	1,5	1.75	2	2.25	2,5	2.75	3
Stress Regime R'_t	Radial EXTENSIVE		Pure EXTENSIVE		TRANSTENSIVE		Pure STRIKE-SLIP		TRANSPRESSIVE		Pure COMPRESSIVE		Radial COMPRESSIVE
Color Scale of R'													
Stress Regime R'_w	0		0.5		1		1.5		2		2.5		3
			Normal Fault (NF)				Strike-Slip Fault				Thrust Fault		

Table 2

The stress inversion results from ten zones within the study area for the 0-15 km depth interval. The column "n" refers to the number of data successfully inverted, while "nt" represents the total number of data before inversion. The reduced stress tensor parameters include the principal stresses: maximum stress (σ1), intermediate stress (σ2), and minimum stress (σ3), each given in terms of plunge and azimuth. Horizontal stress components are represented by maximum horizontal stress (SHmax) and minimum horizontal stress (Shmin), along with the stress ratio (R). The stress regime (R') is defined alongside the stress regime based on the World Stress Map (R'w) and the tensor-based stress regime (R't). Additionally, the table includes misfit, such as the misfit value (αval), the standard deviation of misfit (αStD), and the maximum misfit (αMax). The coefficient of friction (π) is calculated as the arctan of the magnitude of the resolved normal stress (σNmag) divided by the magnitude of the resolved shear stress (τmag) on the plane. Finally, σNmag represents the magnitude of the resolved normal stress, and τmag denotes the magnitude of the resolved shear stress on the plane.

	Zone	Data		Parameter of Reduced Stress Tensor						Horizontal Stress		Stress Ratio			Stress Regime	Misfit			π	σ_{Nmag}	τ_{mag}	QRw
		n	n_t	σ_1 pl	σ_1 azim	σ_2 pl	σ_2 azim	σ_3 pl	σ_3 azim	SH_{max}	Sh_{min}	R	R'	R'_w	R'_t	α_{val}	α_{StD}	α_{Max}				
1	Semangko Fault	6	7	6	341	82	194	4	71	161	71	0,33	1,67	SS	Pure STRIKE-SLIP	13,7	6,5	24,2	28,7	38,2	15,5	C
2	Pelabuhan Ratu	15	15	31	242	57	84	10	338	67	157	0,87	1,13	SS	Extensional STRIKE-SLIP	21,9	14,2	47,3	34,3	58,4	33,7	C
3	Cimandiri Fault	22	22	16	188	56	303	30	89	8	98	0,04	1,96	SS	Compressional STRIKE-SLIP	13,9	12,4	43	34,6	54	30,9	B
4	Baribis Fault	19	21	22	206	11	112	65	357	28	118	0,24	2,24	TF	Strike-slip COMPRESSIVE	10,2	5,8	21,8	36,9	54,3	37	A
5	Lembang Fault	4	5	32	59	57	258	9	154	61	151	0,27	1,73	SS	Compressional STRIKE-SLIP	11,3	4,6	17,5	37,6	54,6	36,5	C
6	Southern Garut	13	14	2	196	15	106	75	293	16	106	0,33	2,33	TF	Pure COMPRESSIVE	19,1	13,8	47,4	30	56,9	32	B
7	West Java South Sea	25	29	1	13	21	103	69	280	13	103	0,04	2,04	TF	Strike-slip COMPRESSIVE	16,8	11,9	41,9	38,2	51,7	36,4	B
8	Sunda Strait Indentation	10	11	1	216	83	118	7	306	36	126	0,76	1,24	SS	Extensional STRIKE-SLIP	19	11,7	37,5	35,5	53,2	30,3	B
9	Mentawai Fault	44	49	15	206	62	87	24	303	27	117	0,14	1,86	SS	Compressional STRIKE-SLIP	17,1	13,3	47,2	35,7	54,6	36,2	B
10.A	Western Sunda Strait	14	14	63	217	20	355	16	91	4	94	0,69	0,69	NF	Pure EXTENSIVE	21,3	13,6	40,3	34,9	53,2	34,3	C
10.B	Eastern Sunda Strait	30	91	21	30	66	243	12	125	34	124	0,81	1,19	SS	Extensional STRIKE-SLIP	14	10,6	34,8	35,3	55,9	36,6	B

The stress regime R′ is described as a function of the stress ratio R, following the classifications in the World Stress Map (WSM) (Zoback 1992), i.e., R′ = R for the normal fault regime (NF), R′ = (2-R) for the strike-slip fault regime (SS), and R′ = (2+R) for the thrust fault regime (TF). Values for the stress regime R′ are categorized as follows: R′ 0-1 are indicative of the normal fault regime (NF), R′ 1-2 are representative of the strike-slip fault regime (SS), and R′ 2-3 are denoted as the thrust fault regime (TF). Specific classifications are R′ 0 for the radial extensive fault regime, R′ 0.5 for the pure normal fault regime, R′ 1 for the transtensive fault regime, R′ 1.5 for the pure strike-slip regime, R' 2 for the transpressive fault regime, R′ 2.5 for the pure thrust fault regime, and R′ 3 for the radial compressive fault regime. Stress regime maps are illustrated using color scales based on (Delvaux & Barth 2010) (Table 1).

Regional geological structure

The map of regional geological structures in the study area is based on previous research (Figure 1): in Lampung dominated by strike-slip faults following the research of Amin et al. (1993) Mangga et al. (1993), Sieh & Natawidjaja (2000), Burhan et al. (1993), Gafoer et al. (1993); in the Sunda Strait dominated by normal faults referring to Susilohadi et al. (2009), Fistria (2016), and Susilohadi (2019); in the Java Sea dominated by N-S oriented subsurface normal faults referring to Asikin et al. (2008); and West Java is dominated by strike-slip and reverse faults based on the research of Sudjatmiko (1972), Silitonga (1973), Sukamto (1975), Santosa (1991), Rusmana et al. (1991), Atmawinata and Abidin (1991), Turkandi et al. (1992), Alzwar et al. (1992), Achdan and Sudana (1992), Abidin and Sutrisno (1992), Dardji et al. (1994), Effendi et al. (1998), Koesmono et al. (1996), Supendi et al. (2018) and Widiyantoro et al. (2022).

Zonation

Earthquake focus mechanism data varies in the study area, which is a structural transition region. The varied data cannot be inverted at once and together to obtain inversion results in the form of consistent stress regimes and stress patterns (Barth 2007). Therefore, it is necessary to group data based on geographical and structural geology conditions (Figure 2). In addition, the determination of zoning also considers the risk of earthquakes in the megathrust segments, which include the forearc basin and accretionary prism in the research area, specifically the Enggano Segment in the Mentawai Fault zone, the Sunda-Banten Segment in the Sunda Strait indentation zone (southern of Sunda Strait) and the West Java Segment in the South Java Sea zone (Irsyam et al. 2017). There are ten zones. One zone is located on the island of Sumatra, zone 1. Semangko Fault: five zones are situated on the island of Java, zone 2. Pelabuhan Ratu, zone 3. Cimandiri Fault, zone 4. Baribis Fault, zone 5. Lembang Fault, and zone 6. Southern Garut: three zones are in the accretionary prism, zone 7. Southern Java Sea, zone 8. Sunda Strait Indentation, and Zone 9. Mentawai Fault: finally, one zone is in the Sunda Strait, divided into zone 10.A. The Western Sunda Strait and Zone 10.B. Eastern Sunda Strait (Figure 2).

RESULTS AND DISCUSSION

Semangko fault (Zone 1)

The Semangko Fault is an active dextral fault representing the southeasternmost segment of the Sumatra Fault Zone on the Sumatra Island. The Sumatra Fault extends for 1,900 km in an NW-SE direction along the western side of Sumatra (Sieh & Natawidjaja 2000). Within the 0-15 km depth interval, the fault displays a strike-slip stress regime with an R' value of 1.67 and a maximum horizontal stress (SH_{max}) oriented at N161°E (SSE-NNW) (Table 2). This R' value reflects a stress ratio of 0.3, approaching 0.5, suggesting a near-equilibrium between compressive and tensile forces. At the 15-33 km depth interval, the stress regime remains strike-slip (R' 1.33) and SH_{max} oriented at N180°E (N-S) (Table 3). A clockwise rotation of SH_{max} by 19° is noted between these depth intervals (Figure 5).

Pelabuhan Ratu (Zone 2)

The Pelabuhan Ratu zone is a tectonic depression formed by normal faulting and is part of the Ujung Kulon Basin in southern Banten (Asikin et al. 2008). At a 0-15 km depth interval, Pelabuhan Ratu demonstrates a transtensive fault stress regime (R' 1.13) and SH_{max} oriented at N67°E (ENE-WSW) (Table 2). Given the orientation of SH_{max} relative to the E-W fault trend, the strike-slip component is interpreted as sinistral, in agreement with observations by Malod (Malod et al. 1995). This interpretation is supported by normal faulting identified through seismic cross-sections (Yulianto et al. 2007), consistent with a stress ratio R 0.87. At the 15-33 km depth interval, the stress regime transitions

to a strike-slip regime (R' 1.67) and SH_{max} oriented at N4°E (N-S) (Table 3), indicating a counterclockwise rotation of SH_{max} by 63° between the 0-15 km and 15-33 km intervals (Figure 5). This analysis suggests the presence of a transtensional fault along the extended section of the Cimandiri Fault.

Cimandiri fault (Zone 3)

The Cimandiri Fault is an active sinistral fault (Dardji 1994; Pulunggono & Martodjojo 1994). Most earthquake focal mechanism data from the western segment of the Cimandiri Fault indicate a predominantly strike-slip fault and reverse fault within the 0-15 km depth interval. A formal stress inversion was performed using 11 focal mechanism data from the 0-15 km interval, while only 3 data were available for the 15-33 km interval, showing a combination of strike-slip and normal faulting mechanisms (Figure 2). At the 0-15 km depth interval, the Cimandiri Fault demonstrates a transpressive stress regime (R' 1.96) and SH_{max} oriented at N8°E (N-S) (Table 2). This N-S orientation of SH_{max} is consistent with findings by Tingay et al. (2012). The stress ratio R-value, close to zero (R 0.04), indicates a predominance of compressional stress within the Cimandiri Fault, particularly in its western segment. Marliyani et al. (2016) support the transpressive stress regime and describe the Cimandiri Fault as a strike-slip fault with dominant reverse dip-slip movement. However, the low stress ratio (R 0.04) and the orthogonal convergence in Java suggest that the Cimandiri Fault likely behaves as a reverse fault, with reverse dip-slip being more prominent than strike-slip. Several researchers (Bemmelen 1949; Hall et al. 2007; Clements et al. 2009; Haryanto et al. 2017) have classified the Cimandiri Fault as a strike-slip fault. An anomaly was identified within the depth interval of 15–33 km, marked by a change in the stress regime (R') to a transtensive fault stress regime with R' = 0.98 and SH_{max} oriented N18°E (N-S) (Figure 5).

This anomaly is associated with two earthquake mechanisms: strike-slip faulting and normal faulting. The transtensive stress regime anomaly is interpreted to result from slab pull forces exerted by the subduction of the Indo-Australian Plate, causing vertical stress to dominate over horizontal stress. Based on the orientation of SH_{max} relative to the alignment of the Cimandiri Fault, the fault movement is interpreted as sinistral (left-lateral).

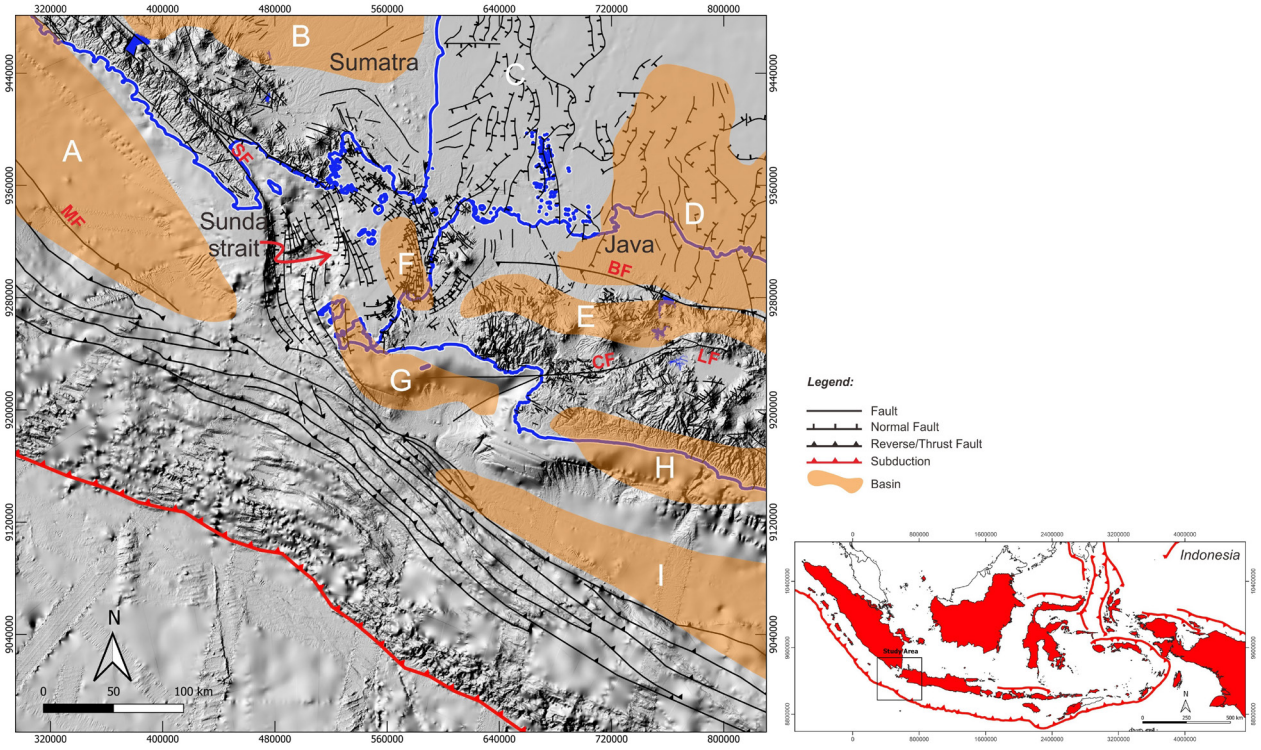

Figure 1
Map of regional geological structures in the study area. Mentawai Fault (MF) (Diament et al. 1992), Semangko Fault (SF) (Sieh & Natawidjaja 2000), Baribis Fault (BF) (Widiyantoro et al. 2022); Cimandiri Fault (CF) (Dardji et al. 1994), and Lembang Fault (LF) (Tjia 1968; Hidayat 2010; Daryono et al. 2019). The orange color is a basin based on (Asikin et al. 2008a): (A) Bengkulu Basin, (B) South Sumatra Basin, (C) Sunda Basin, (D) Northwest Java Basin, (E) Bogor Basin, (F) Sunda Strait Basin, (G) Ujung Kulon Basin, (H) South of West Java Basin, (I) South Java Basin.

 | DOI.org/10.29017/scog.v48i1.1687

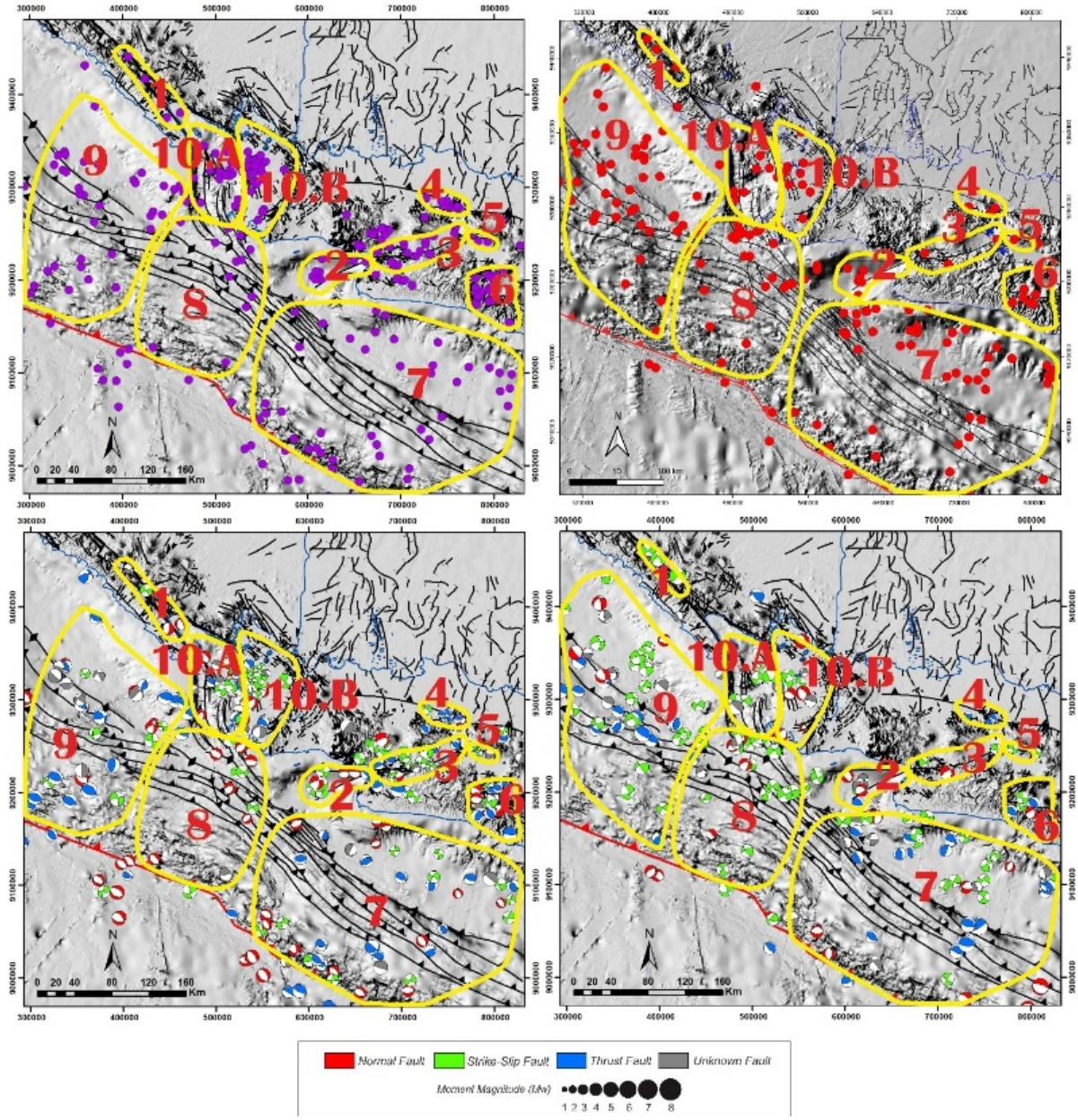

Figure 2
Zones 1-10 and earthquake focal mechanism data distribution in the 0-15 km (left) and 15-33 km (right) depth intervals. This data includes various types of faults: normal faults (red beachballs), strike-slip faults (green beachballs), thrust faults (dark blue beachballs), and 'odd' faults (gray beachballs) with the scale of moment magnitudes.

Baribis fault (Zone 4)

Recent studies classify the Baribis Fault as part of the West Java Back-arc Thrust (WJBT), dated to the Pliocene (Aribowo et al. 2022)but the faults' nature, timing, and activity remain partly elusive. Characterizing the structure and activity of the seismogenic Java Back-arc Thrust (historical earthquakes up to 7 Mw. The Baribis Fault is primarily a reverse fault (Haryanto 1999) with a dominant reverse slip (Widiyantoro et al. 2022). Yet, sinistral movement has also been identified, with rupture displacements measuring 5 ± 1 m (Daryono et al. 2021)including Cirebon, Indramayu, Sumedang, and Subang area (with a probability of continuing to Jakarta and Banten areas.

Focal mechanism data for earthquakes along the Baribis Fault primarily utilize the data of (Widiyantoro et al. 2022), with events of moment magnitude < Mw 3.2. The earthquake mechanisms from beachball diagrams indicate that the Baribis Fault is a reverse fault with a minor strike-slip component. At the 0-15 km depth interval, the

Baribis Fault exhibits a transpressive stress regime (R' 2.24) with SH_{max} oriented at N28°E (NNE-SSW) (Table 2), approaching a thrust fault stress regime (R' 2.25). In this interval, the fault movement is interpreted as sinistral, with a dominant reverse slip component over strike-slip. The stress regime remains transpressive (R' 2.0) in the 15-33 km depth interval and SH_{max} oriented at N38°E (Table 3).

Lembang fault (Zone 5)

The Lembang Fault, which extends 29 km (Daryono et al. 2019), runs from Padalarang to Mount Palasari in a west-east direction. Interpretations of the Lembang Fault's movement vary, with some researchers classifying it as a normal fault (Hidayat 2010; Aribowo et al. 2022; Agustya 2018), a reverse fault (Agustya 2018), or a sinistral fault (Supendi et al. 2018; Tjia 1968; Daryono et al. 2019; Meilano et al. 2012; Hussain et al. 2023).

Most earthquake focal mechanism data for the Lembang Fault come from Supendi (Supendi et al. 2018), who indicate a strike-slip fault mechanism. At 0-15 km depth, the fault exhibits a strike-slip stress regime (R' 1.73) with SH_{max} oriented at N61°E (ENE-WSW) (Table 2). Similarly, the stress regime remains strike-slip at 15-33 km depth (R' 1.5) (Table 3). The stress ratio R across both depth intervals ranges from 0.27 to 0.33, indicating a slight compressional component. It suggests that while the Lembang Fault primarily displays strike-slip movement, a minor reverse-slip component exists with compressional strike-slip stress tensors. Based on SH_{max} orientation at 0-15 km and 15-33 km depths, oriented at N40°E (NE-SW) relative to the E-W alignment of the Lembang Fault, the fault is interpreted as sinistral. The SH_{max} orientation along the Lembang Fault aligns with (Tjia 2001), who noted a NE-SW orientation, and with (Marliyani et al. 2020), who identified major tectonic stress directions in the region through volcanic morphology analysis at Mount Tangkuban Perahu.

At the 0-15 km depth interval (Figure 5), SH_{max} along the three active faults (Cimandiri, Baribis, and Lembang Faults) exhibits rotational patterns. From the Cimandiri Fault to the Baribis Fault, SH_{max} rotates clockwise by 20°. A further clockwise SH_{max} rotation of 53° is observed between the Cimandiri and Lembang Faults, while the rotation from the Baribis to the Lembang Fault is 33°. In contrast, at the 15-33 km depth interval, SH_{max} rotation is smaller, displaying a more parallel and consistent pattern than the 0-15 km depth. Between the Cimandiri and Baribis Faults, SH_{max} rotates counterclockwise by 20°, while from the Baribis to the Lembang Fault, it rotates clockwise by only 2°. The SH_{max} rotation from the Cimandiri to the Lembang Fault is 22°. These variations reflect data heterogeneity across West Java, particularly within these three active faults.

Southern Garut (Zone 6)

The Southern Garut Zone (SGZ) is characterized by its active seismicity, particularly along the Garsela Fault, which trends NE-SW (Arisbaya et al. 2021). The earthquake focal mechanism data for the Southern Garut Zone (Zone 7) exhibit significant heterogeneity. The stress inversion results provide insights relevant to the regional geological framework, and we present the orthogonal tectonic implications for Java to achieve a more uniform and stable representation of the stress field. At depths ranging from 0-15 km within the Southern Garut Zone, a reverse fault stress regime (R' 2.33) is observed, with the maximum horizontal stress (SH_{max}) oriented at N16°E (NNE-SSW) (Table 2). Conversely, at depths between 15-33 km, the stress regime transitions to a transpressive fault stress regime (R' 1.78), with SH_{max} oriented at N48°E (NE-SW) (Table 3).

Considering the heterogeneity in the earthquake focal mechanism data, this zone displays anomalous stress fields and regimes. During the formal stress inversion process, a subset of the data indicated a radial extensional stress regime (R' 0.13) with SH_{max} aligned at N99°E (W-E). This orientation does not correspond with the predominant NE-SW and NW-SE geological structures, nor with the orthogonal tectonic setting of Java, where the overall SH_{max} trend is NNE-SSW. Consequently, this particular subset was excluded from the analysis. The observed stress anomalies in the Southern Garut Zone warrant further investigation in future research endeavors.

West Java South Sea (Zone 7)

In the southern offshore area of West Java, within a depth range of 0-15 km, the stress regime is dominated by a thrust fault stress regime (R' 2.04), with a SH_{max} oriented at N13°E (NNE-SSW) (Table 2). This stress regime persists in the deeper interval from 15 to 33 km, displaying a thrust fault regime (R' 2.26) with SH_{max} oriented at N24°E (NE-SW) (Table 3). Both the SH_{max} orientation and the stress regime in the southern offshore region of West Java align with the results reported by Pratama & Kita (2022).

Table 3
Stress inversion results of the ten zones in the study area for the depth interval 15-33 km. Table information can be seen in table 2

	Zone	Data		Parameter of Reduced Stress Tensor						Stress Horizontal		Rasio Stress			Stress Regime	Misfit			π	σ_{Nmag}	τ_{mag}	QRw
		n	n_t	σ_1 pl	σ_1 azim	σ_2 pl	σ_2 azim	σ_3 pl	σ_3 azim	SH_{max}	Sh_{min}	R	R'	R'_w	R'_t	α_{val}	α_{StD}	α_{Max}				
1	Semangko Fault	5	5	19	178	69	22	8	271	180	90	0,67	1,33	SS	Pure STRIKE-SLIP	5,7	5,3	11,9	37,1	56	41,4	C
2	Pelabuhan Ratu	13	17	22	180	51	60	30	284	4	94	0,33	1,67	TS	Oblique TRANSPRESSIVE	19,7	13,6	42,1	35,2	56,9	38,3	B
3	Cimandiri Fault	5	5	55	86	10	191	33	288	18	108	0,98	0,98	NF	Strike-slip EXTENSIVE	1,4	0,6	2,3	39,3	48,7	30,5	C
4	Baribis Fault	5	5	4	218	21	126	68	319	38	128	0	2	TF	Strike-slip COMPRESSIVE	1,4	0,6	2,3	39,3	48,7	30,5	C
5	Lembang Fault	3	3	6	41	71	149	18	309	40	130	0,33	1,5	SS	Pure STRIKE-SLIP	16	4	20,8	41,7	48,2	40,3	C
6	Southern Garut	10	11	27	49	60	203	11	313	48	138	0,22	1,78	SS	Compressional STRIKE-SLIP	11	9,5	30,6	31,6	45,9	27,6	B
7	West Java South Sea	37	43	13	203	14	110	71	335	24	114	0,26	2,26	TF	Pure COMPRESSIVE	15,4	10,8	43,3	34,9	53,2	31,5	B
8	Sunda Strait Indentation	38	42	7	203	83	21	0	113	23	113	0,46	1,54	SS	Pure STRIKE-SLIP	11,8	10,1	45,2	36,2	54	36,4	A
9	Mentawai Fault	55	66	27	214	5	306	63	46	34	124	0,12	2,12	TF	Strike-slip COMPRESSIVE	11,4	10,4	40	35,6	54,8	38,6	A
10.A	Western Sunda Strait	25	25	14	205	76	22	1	114	25	115	0,57	1,43	SS	Pure STRIKE-SLIP	18,2	17,6	68,5	35,0	54,7	35,0	B
10.B	Eastern Sunda Strait	12	21	79	86	8	307	7	216	122	32	0,2	0,2	NF	Radial EXTENSIVE	19,4	12	38,3	34,8	55,7	33,8	B

Sunda strait indentation (Zone 8)

The Sunda Strait indentation forms part of the Sunda Strait-Banten megathrust segment (Irsyam et al. 2017), which can generate a large earthquake with an estimated maximum magnitude of up to Mw 8.9. This high potential is attributed to a seismic gap with lower seismic activity than surrounding regions (Rahman et al. 2021; Supendi et al. 2023) but further effort is required to help understand both the likelihood and frequency of such events. With this in mind, we exploit catalog seismic data sourced from the Agency for Meteorology, Climatology, and Geophysics (BMKG. This seismic gap suggests strain accumulation within the subduction interface, which could be released as substantial energy during a major earthquake (Supendi et al., 2023) but further effort is required to help understand both the likelihood and frequency of such events. With this in mind, we exploit catalog seismic data sourced from the Agency for Meteorology, Climatology, and Geophysics (BMKG. Numerous studies have investigated this seismic gap in the Sunda Strait indentation (e.g., Octonovrilna et al. 2018; Widiyantoro et al. 2020; Rahman et al. 2021; Supendi et al. 2023). At a 0–15 km depth interval, the stress regime is characterized by a thrust fault regime with R' = 1.24 and SH_{max} oriented N36°E (NE-SW) (Table 2). At a deeper interval of 15–33 km, the stress regime transitions to a strike-slip fault regime with R' = 1.54 and SH_{max} oriented N23°E (NE-SW) (Table 2).

Mentawai fault (Zone 9)

The Mentawai Fault in this zone trends NW-SE and extends approximately 500 km. It was first identified by (Diament et al. 1992) through seismic reflection profile analysis, which revealed a favorable flower structure. In zone 9, the distribution of earthquake focal mechanisms is mainly concentrated within the fore-arc ridge, fore-arc basin, and their boundary, where both thrust and strike-slip faulting mechanisms are observed. At 15–33 km depths, strike-slip fault mechanisms become more prevalent in this zone. The occurrence of strike-slip faults here is attributed to the oblique subduction of the Indo-Australian Plate beneath Sumatra, generating numerous strike-slip faults, including Sumatra's two major faults: the Sumatra Fault and the Mentawai Fault with the same orientation (NW-SE) and the same sense of movement (dextral). In zone 9, the Mentawai Fault area displays a transpressive stress regime (R' 1.86) at depths of 0–15 km, and SH_{max} oriented at N27°E (NE-SW) (Table 2). This stress regime is consistent at 15–33 km depths, characterized by a transpressive stress regime (R' 2.12) and SH_{max} oriented at N34°E (NE-SW) (Table 3). The principal stress direction, σ_1, derived from stress inversion within the Mentawai Fault Zone, is oriented at 15°/N206°E at depths of 0–15 km and 27°/N214°E at 15–33 km, generally aligning in an NE-SW orientation (Figure 3 and Figure 4). This orientation corresponds with the NE-SW trend (Shamim et al. 2019) reported in Zone VI (in his publication), which encompasses southern Sumatra and the Mentawai Fault Zone.

Sunda strait (Zone 10.A and 10.B)

The initiation of the opening of the Sunda Strait occurred in the Late Miocene, following the formation of the Sumatra Fault during the Early Miocene (Susilohadi et al. 2009). The Sunda Strait was formed due to the dextral movement of the Sumatra Fault (Bemmelen 1970), along with the northwestward movement of the Sumatra forearc sliver block, which caused extensional deformation in the Sunda Strait and its adjacent southern sea (Huchon & Pichon 1984; Jarrard 1986; Susilohadi et al. 2009; Diament et al. 1992; Diament et al. 1990).

The Sunda Strait comprises two main basins: the Eastern and Western Sunda Strait Basin (Pramumijoyo & Sebrier 1991). A formal stress inversion was conducted for the Western Sunda Strait (Zone 10.A) and the Eastern Sunda Strait (Zone 10.B) based on the basin subdivision by Pramumijoyo and Sebrier (1991). Numerous earthquakes at depths of 0-15 km and 15-33 km indicate that the faults within the Sunda Strait are active, particularly in the Western Sunda Strait Basin, which is more actively opening and expanding (Pramumijoyo & Sebrier 1991). In the Western Sunda Strait (Zone 10.A), at a depth range of 0-15 km, a normal faulting stress regime (R' 0.69) and SHmax oriented N4°E (N-S) (Table 2). In contrast, Zone 10.B in the Eastern Sunda Strait at the same depth range exhibits two stress regimes in two subsets: a transtensive fault (R' 1.19) and SH_{max} oriented N34°E (NE-SW) (Table 2) and a strike-slip fault (R' 1.31) and SHmax oriented N114°E. At depths of 15-33 km, the Western Sunda Strait shows a strike-slip stress regime (R' 1.43) and SHmax oriented N25°E. However, in this model, the most relevant subset for the regional geological conditions is the subset characterized by a transtensive fault regime. Meanwhile, the Eastern Sunda Strait at the same depth range displays an extensive stress regime (R' 0.2) and SH_{max} oriented N122°E.

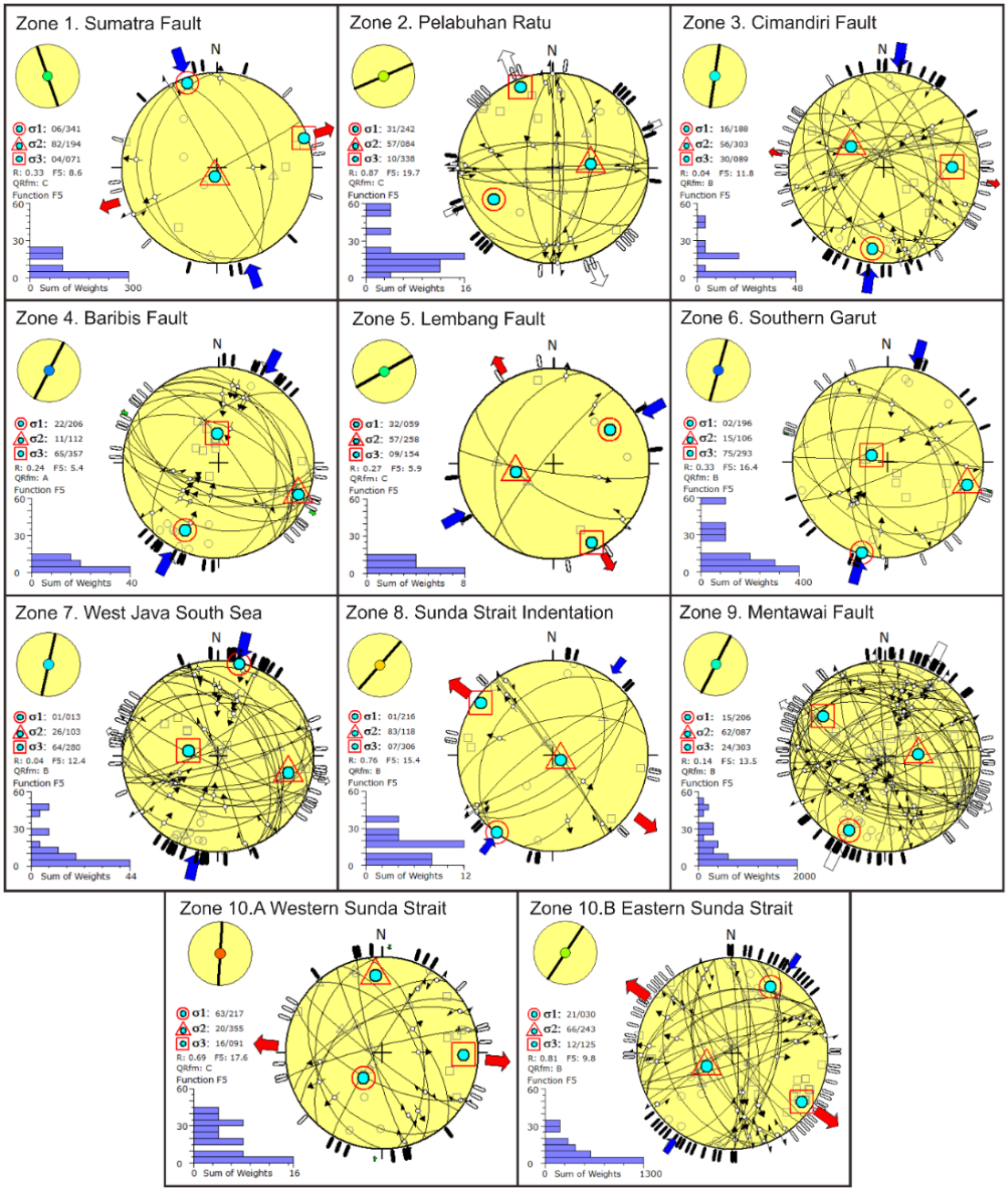

Figure 3

Stress inversion results of rotational optimization method in zones 1-10 of the 0-15 km depth interval. σ1 represents the primary stress and is depicted with a circular symbol, σ2 indicates the intermediate stress with a triangle symbol, and σ3 is the lowest stress, symbolized by a square. The maximum horizontal stress (SHmax) is marked by short black lines around the outer edge of the stereogram, while short white lines show the minimum horizontal stress (Shmin). These SHmax and Shmin lines are oriented perpendicularly to one another. The stress tensor is illustrated by a small circle with an arrow at the top left, which provides information about the magnitude of horizontal deviatoric stress about stress isotropy (σi). The characteristics of the arrow—its type, size, and color—represent the magnitude of stress and are linked to the stress regime R' and stress ratio R = (σ2 – σ3) / (σ1 – σ3). A red arrow indicates that σ3 is nearly horizontal (Shmin), a green arrow signifies that σ2 is nearly horizontal (either Shmin or SHmax), and a blue arrow shows that σ1 is nearly horizontal (always SHmax). Outward arrows suggest extensional deviatoric stress (< σi), whereas inward arrows indicate compressional deviatoric stress (> σi). Vertical stress is displayed as either a filled or outlined circle at the center of the diagram. A red-filled circle suggests an extensional stress regime (σ_1≈σ_v), a green-filled circle represents a strike-slip regime (σ_2≈σ_v), and a dark blue-filled circle indicates a compressional regime (σ_3≈σ_v). Open arrows and circles imply oblique stress axes. The parameter R is the stress ratio. F5 is a key function that minimizes the difference between observed slip and calculated slip vectors on the fault plane, maximizes the resolved shear stress, and reduces the resolved normal stress. A lower F5 value indicates a better match with the true slip plane of one of the nodal planes and yields a more accurate stress tensor. The symbols for squares, circles, and triangles in the stereogram reflect the orientation of the kinematic axes.

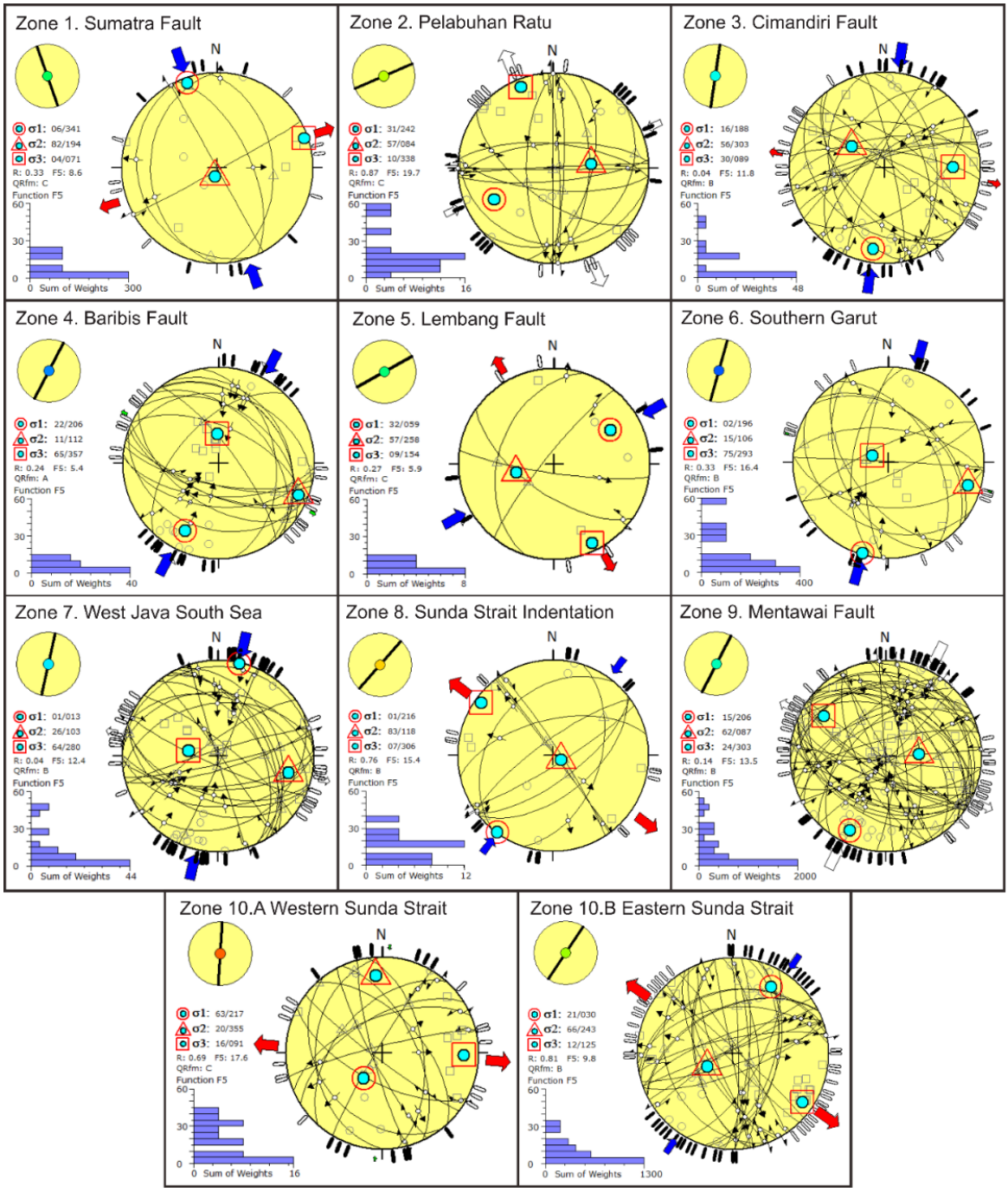

Figure 4
Stress inversion results of rotational optimization method in zones 1-10 of the 15-33 km depth interval. Explanation of the picture can be seen in the description of Figure 4

Tectonic stress regime in Lampung, Sunda strait and West Java

There are notable differences in stress regimes (R') across Lampung, the Sunda Strait, and West Java. Based on stress inversion analysis across 10 zones at a depth interval of 0–15 km, the average stress regimes ($\bar{R}'$) in these three regions indicate that Lampung, representing Sumatra, is dominated by a strike-slip stress regime ($\bar{R}'$ 1.67); the Sunda Strait displays a transtensive stress regime ($\bar{R}'$ 0.94); and West Java experiences a thrust fault stress regime ($\bar{R}'$ 1.87). At a deeper interval of 15–33 km, the average stress regimes ($\bar{R}'$) are as follows: Lampung with a strike-slip fault regime ($\bar{R}'$ 1.33); the Sunda Strait with a transtensive regime ($\bar{R}'$0.82); and West Java with a strike-slip regime ($\bar{R}'$1.59). The average stress regimes in Lampung and the Sunda Strait remain relatively stable across both depth intervals (Figures 6), consistent with Sumatra's oblique convergence, which induces strike-slip faulting. This tectonic influence also extends to the Sunda Strait, where Sumatra's tectonic dynamics sustained a transtensive stress regime. In contrast, West Java exhibits a shift in average stress regime ($\bar{R}'$) between the 0–15 km and 15–33 km depth intervals. This shift corresponds with Java's tectonic setting, where orthogonal convergence leads to thrust faulting near the surface, while deeper faults transition to strike-slip faulting.

Horizontal stress and its implications for fracture geomechanics

The pattern of maximum horizontal stress (SH_{max}) in the structural transition zone between Sumatra and Java exhibits distinct variations and rotations in the SH_{max} orientation, with the Sunda Strait acting as a boundary zone. In the fore-arc ridge south of Sumatra, SH_{max} is oriented NE-SW, but it rotates counterclockwise across Sumatra to an NW-SE orientation. This shift in stress orientation reflects a stress distribution influenced by strain partitioning due to the oblique convergence of the Indo-Australian and Eurasian plates. In the Sunda Strait, the SH_{max} direction shows considerable variation, including N-S, NE-SW, and W-E orientations. (Figure 5).

In reservoir geomechanics, the patterns of SH_{max} and Sh_{min} are crucial for optimizing hydrocarbon production, both by modeling or predicting natural fractures beneath the surface and determining the optimal orientation for horizontal wells. A thorough understanding of these horizontal stress patterns enables the identification of more efficient hydrocarbon flow pathways and the design of well placements to enhance productivity. SH_{max} typically aligns with open fractures, serving as primary

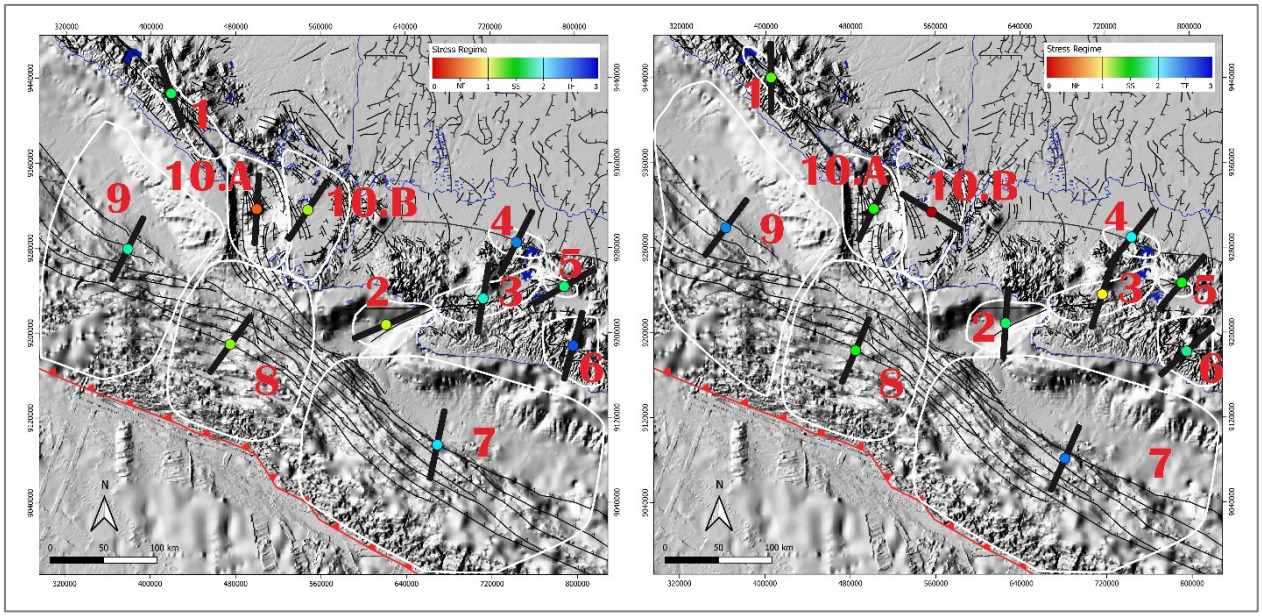

Figure 5
The stress regime map and SH_{max} orientation obtained from stress inversion are illustrated for zones 1 through 10. (Left) presents the stress regime map for the 0–15 km depth interval, while (Right) depicts the stress regime map for the 15–33 km depth interval. In each zone, the maximum horizontal stress (SH_{max}) is indicated by black bars, representing azimuthal orientation ranging from 0° to 360°. The circle positioned at the midpoint of each SH_{max} bar denotes the color index for the stress regime R', as specified by the color scale in the upper-right corner of the figure.

conduits for hydrocarbon flow (Aiman et al. 2023). In reservoir development, SH_{max} orientation optimizes wellbore placement and hydraulic fracturing design (Logue 2015). Horizontal well performance is often influenced by stress redistribution, primarily controlled by the boundaries of geological structures due to variations in elastic properties within the subsurface (Widarsono 2000). Proper evaluation of horizontal well performance is essential before drilling decisions to ensure that the anticipated improvement in well productivity justifies the associated drilling and completion costs compared to vertical wells (Tunggal 2000). Furthermore, well control simulators for vertical and horizontal wells can be valuable tools in drilling planning and evaluation, providing critical insights into well management during and after drilling operations (Purnomo & Tobing 2007). Understanding in situ stress plays a pivotal role in petroleum exploration and production, as it enhances the ability to interpret modern deformation patterns within sedimentary basins, offering valuable insights into subsurface conditions (Ramdhan 2021). As in horizontal well drilling, when the well trajectory aligns with Shmin, transverse fractures (perpendicular to the well) are formed, whereas wells aligned with SH_{max} produce longitudinal fractures (parallel to the well) (Yang 2014; Mohamed et al. 2016a). Wells drilled in the direction of Shmin (on-azimuth) typically yield higher hydrocarbon production than those drilled perpendicular to Shmin (Rostami et al. 2020).

The stress pattern used to predict the orientation of open fractures in the tertiary basin reservoirs within the study area is based on the SH_{max} orientation at depths of 0–15 km. The stress trajectory map for this depth range was constructed by interpolating SH_{max} orientations obtained from stress inversion analysis (Figure 7). In the Bengkulu Basin, the SH_{max} trajectories predominantly trend NE-SW and N-S. These directions are interpreted as the general orientation of open fractures, including naturally formed and hydraulically induced fractures. The optimal direction for horizontal drilling follows the Sh_{min} orientation, which is NW-SE.

In the South Sumatra Basin and Sunda Basin, no earthquake focal mechanism data are available, and thus, the SH_{max} orientation remains undetermined. In the Northwest Java Basin, the SH_{max} trajectories trend NE-SW, but this pattern is only observed in the southern part of the basin, bounded by the Baribis Fault. While the maximum horizontal stress (SH_{max}) orientation is uncertain further north, it is inferred that the shift to a north-south direction should be based on the normal fault orientations in West Java's northern offshore region. Consequently, open fractures are interpreted to trend NE-SW and N-S, while the optimal direction for horizontal drilling is W-E. In the Bogor Basin and Southern West Java Basin, the SH_{max} trajectories trend NE-SW, which is also interpreted as the orientation of open fractures. The optimal direction for horizontal drilling aligns with the Sh_{min} orientation, namely NW-SE and W-E. In the Southern Java Basin, the SHmax orientation trends NE-SW and N-S are interpreted as open fracture orientations. Meanwhile, in the Sunda Strait Basin and Ujung Kulon Basin, the SH_{max} orientation is relatively consistent at NE-SW, indicating that open fractures are also oriented NE-SW. The optimal direction for horizontal drilling in these basins aligns with the Sh_{min} orientation, NW-SE.

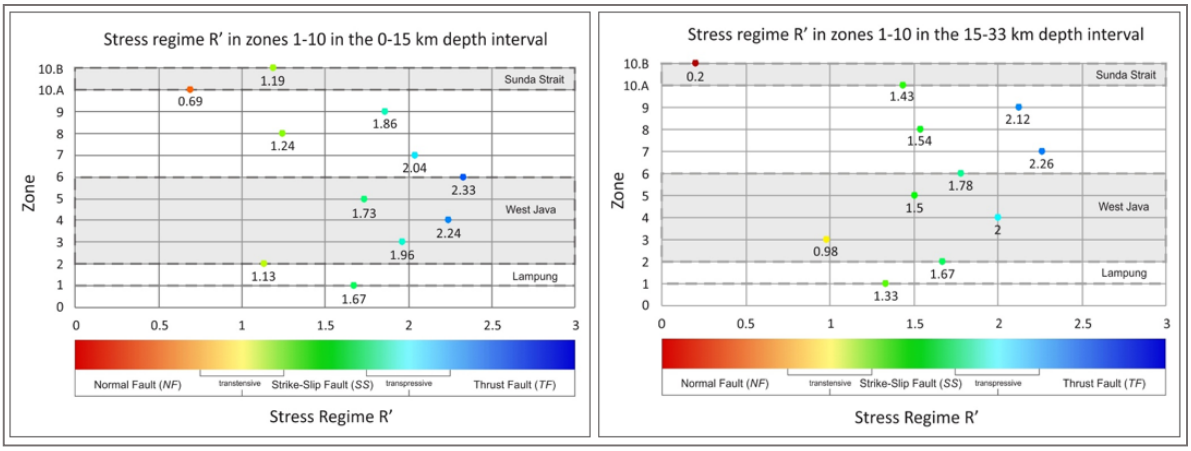

Figure 6
The average stress regime ($\overline{(R')}$) across ten zones at a depth interval of 0-15 km (left) and 15-33 km (right). The colored circles represent the color index of the stress regime R'.

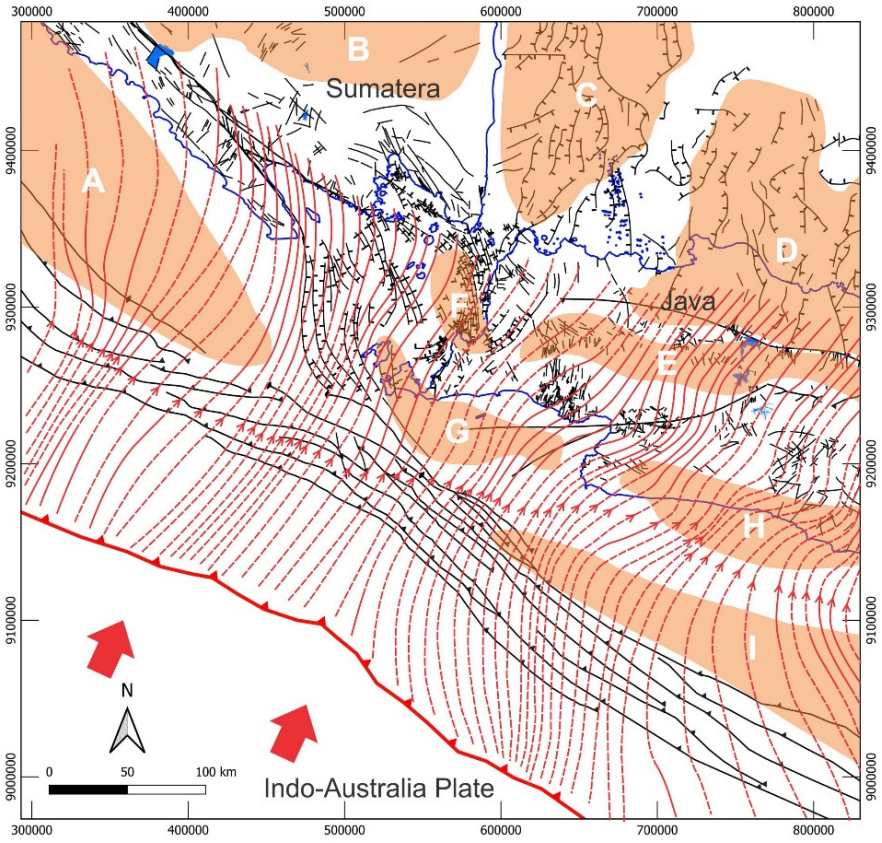

Figure 7
SHmax patterns and trajectories in the research area. Solid or dashed red lines are stress trajectories. The orange color is a basin based on Asikin et al. (2008a): (A) Bengkulu Basin, (B) South Sumatra Basin, (C) Sunda Basin, (D) Northwest Java Basin, (E) Bogor Basin, (F) Sunda Strait Basin, (G) Ujung Kulon Basin, (H) South of West Java Basin, (I) South Java Basin.

CONCLUSION

There are distinct differences in the stress regimes within this structural transition zone. In Sumatra, the average stress regime is dominated by a strike-slip regime (1.67) at depths of 0–15 km and 1.33 at depths of 15–33 km, primarily influenced by the oblique convergence of the Indo-Australian Plate against Sumatra. In the Sunda Strait, a transtensive stress regime is observed, with values of 0.94 at depths of 0–15 km and 0.82 at depths of 15–33 km, where Sumatra's tectonic activity continues to impact the stress regime. In West Java, a thrust fault regime is evident at depths of 0–15 km, with 1.87, transitioning to a strike-slip regime with 1.59 at depths of 15–33 km. This variation is shaped by Java's tectonic setting, where the orthogonal convergence of the Indo-Australian Plate against Java exerts a significant influence.

The stress trajectories crossing the Tertiary basin indicate the orientation of open fractures, particularly within the reservoir rocks. Open fractures can form naturally or through hydraulic fracturing processes that align with SH_{max}. In West Java and the Sunda Strait, open fractures are generally interpreted to have an NE-SW orientation, transitioning to an N-S orientation in the northern offshore areas of West Java. Meanwhile, open fractures in the Lampung region are predominantly interpreted to exhibit an N-S orientation.

ACKNOWLEDGEMENTS

Special thanks to Prof. Benyamien Sapiie, Ph.D who always supports, helps and motivates the author. Thank you for the BPP-DN (Domestic Postgraduate Scholarships) scholarship from Indonesia's Kemenristek Dikti (Ministry of Higher Education, Science, and Technology Education).

GLOSSARY OF TERMS

Symbol	Definition	Unit
R	Stress ratio	
R'	Stress regime	
$\bar{R}$'	Average of stress regime	
SH_{max}	Maximum horizontal stress	
Sh_{min}	Minimum horizontal stress	
σ_1	Maximum principal stress	
σ_2	Intermediate principal stress	
σ_3	Minimum principal stress	
NE-SW	Northeast-Southwest	
NW-SE	Northwest-Southeast	
W-E	West-East	
NNE-SSW	North-Northeast – South-Southwest	
SSE-NNW	South-Southeast – North-Northwest	
N-S	North – South	
ENE-WSW	East-Northeast – West-Southwest	

REFERENCES

Abidin & Sutrisno, 1992, Peta geologi lembar Pamanukan, Jawa. Pusat Penelitian dan Pengembangan Geologi.

Achdan, A. & Sudana, D., 1992, Peta geologi lembar Karawang, Jawa. Pusat Penelitian dan Pengembangan Geologi.

Agustya, G., 2018, Geologi daerah Binangun dan sekitarnya, Kecamatan Karanggayam, Kabupaten Kebumen, Jawa Tengah dan studi struktur Sesar Lembang daerah Gunung Batu Kecamatan Lembang, Kabupaten Bandung Barat, Jawa Barat. Universitas Pakuan.

Aiman, Y.A., Delorey, A., Lu, Y. & Bokelmann, G., 2023, SH_{max} orientation in the Alpine region from observations of stress-induced anisotropy of nonlinear elasticity. Geophysical Journal International, 235. https://doi.org/10.1093/gji/ggad353.

Alzwar, A., Akbar, N. & Bachri, S., 1992, Peta geologi lembar Garut dan Pameungpeuk, Jawa. Pusat Penelitian dan Pengembangan Geologi.

Amin, T. C., Sidarto, Santosa, S. & Gunawan, W., 1993, Peta geologi lembar Kotaagung, Sumatera.

Aribowo, S., Husson, L., Natawidjaja, D.H., Authemayou, C., Daryono, M.R., Puji, A.R., Valla, P.G., Pamumpuni, A., Wardhana, D.D., de Gelder, G., Djarwadi, D. & Lorcery, M., 2022, Active Back-Arc Thrust in North West Java, Indonesia. Tectonics, 41(7), e2021TC007120. https://doi.org/https://doi.org/10.1029/2021TC007120.

Arisbaya, I., Lestiana, H., Mukti, M.M., Handayani, L., Grandis, H., Warsa, W. & Sumintadireja, P., 2021, Garsela Fault and other NE-SW active faults along the southern part of Java Island. IOP Conference Series: Earth and Environmental Science, 789, 12065. https://doi.org/10.1088/1755-1315/789/1/012065.

Asikin, S., Sapiie, B., Noeradi, D., Koesoemadinata, Martodjojo, S., Katili, J.A., Satyana, A.H., Luthfi, A., Yulian, B., M.T. Ibrahim, A., Hadianto, K., I. Abdullah, C., Harsolumakso, A.H., Soeminantadireja, P., Ryadi, S., Guntoro, A., Sunardi, E., Prasetyadi, C., Subagio & N. Mulyati, 2008a, Peta cekungan sedimen tersier Indonesia. BP migas, LAPI ITB.

Asikin, S., Sapiie, B., Noeradi, D., Koesoemadinata, Martodjojo, S., Katili, J.A., Satyana, A.H., Luthfi, A., Yulian, B., M.T. Ibrahim, A., Hadianto, K., I. Abdullah, C., Harsolumakso, A.H., Soeminantadireja, P., Ryadi, S., Guntoro, A., Sunardi, E., Prasetyadi, C., Subagio & N. Mulyati, 2008b, Peta tetonik dan struktur Indonesia. BP migas, LAPI ITB.

Atmawinata, S. & Abidin, H.Z., 1991, Peta geologi lembar Ujung Kulon, Jawa Barat. Pusat Penelitian dan Pengembangan Geologi.

Barth, A., 2007, Frequency sensitive moment tensor inversion for light to moderate magnitude earthquakes in eastern Africa and derivation of the regional stress field [Universitat Karlsruhe]. https://doi.org/10.5445/IR/1000005857.

Bott, M.H.P., 1959, The mechanics of oblique slip faulting. Geological Magazine, 96(2), 109–117. https://doi.org/10.1017/S0016756800059987.

Budiarto, 1976, Sunda Strait: a dividing line between tertiary structural patterns in Sumatra and Java islands (pp. 11–20).

Burhan, G., Gunawan, W. & Noya, Y. (1993). Peta geologi lembar Menggala, Sumatera. Pusat Penelitian dan Pengembangan Geologi.

Carton, H., Singh, S.C., Hananto, N.D., Martin, J., Djajadihardja, Y.S., Udrekh, Franke, D. &

Gaedicke, C. (2014). Deep seismic reflection images of the Wharton Basin oceanic crust and uppermost mantle offshore Northern Sumatra: Relation with active and past deformation. Journal of Geophysical Research: Solid Earth, 119(1), 32–51. https://doi.org/https://doi.org/10.1002/2013JB010291

Clements, B., Hall, R., Smyth, H. R., & Cottam, M. A. (2009). Thrusting of a volcanic arc: A new structural model for Java. Petroleum Geoscience, 15(2), 159–174. https://doi.org/10.1144/1354-079309-831

Dardji, N., Villemin, T., & Rampnoux, J. P. (1994). Paleostresses and strike-slip movement: the Cimandiri Fault Zone, West Java, Indonesia. Journal of Southeast Asian Earth Sciences, 9(1–2), 3–11. https://doi.org/10.1016/0743-9547(94)90061-2

Daryono, M. R., Natawidjaja, D. H., Puji, A. R., & Aribowo, S. (2021). Fault rupture in Baribis Fault possibly related to the 1847 major earthquake event in the Cirebon area. IOP Conference Series: Earth and Environmental Science, 873(1), 12052. https://doi.org/10.1088/1755-1315/873/1/012052

Daryono, M. R., Natawidjaja, D. H., Sapiie, B., & Cummins, P. (2019). Earthquake geology of the Lembang Fault, West Java, Indonesia. Tectonophysics, 751, 180–191. https://doi.org/10.1016/j.tecto.2018.12.014

Delvaux, D., & Barth, A. (2010). African stress pattern from formal inversion of focal mechanism data. Tectonophysics, 482(1–4), 105–128. https://doi.org/10.1016/j.tecto.2009.05.009

Delvaux, D., Moeys, R., Stapel, G., Petit, C., Levi, K., Miroshnichenko, A., Ruzhich, V., & San'kov, V. (1997). Paleostress reconstructions and geodynamics of the Baikal region, Central Asia, Part 2. Cenozoic rifting. Tectonophysics, 282(1–4), 1–38. https://doi.org/10.1016/S0040-1951(97)00210-2

Delvaux, D., & Sperner, B. (2003). New aspects of tectonic stress inversion with reference to the TENSOR program. Geological Society Special Publication, 212(January 2003), 75–100. https://doi.org/10.1144/GSL.SP.2003.212.01.06

Diament, M., Harjono, H., Karta, K., Deplus, C., Dahrin, D., Zen, M. T. J., Gerard, M., Lassal, O., Martin, A., & Malod, J. (1992). Mentawai Fault Zone off Sumatra: a new key to the geodynamics of western Indonesia. Geology, 20(3), 259–262. https://doi.org/10.1130/0091-7613(1992)020<0259:MFZOSA>2.3.CO;2

Dokht, R. M. H., Gu, Y. J., & Sacchi, M. D. (2018). Migration Imaging of the Java Subduction Zones. Journal of Geophysical Research: Solid Earth, 123(2), 1540–1558. https://doi.org/https://doi.org/10.1002/2017JB014524

Effendi, A. C., Kusnama, & Hermanto, B. (1998). Peta geologi lembar Bogor, Jawa. Pusat Penelitian dan Pengembangan Geologi.

Fistria, C. I. (2016). Evolusi struktur daerah Selat Sunda. Institut Teknologi Bandung.

Gafoer, S., Amin, T. C., & Pardede, R. (1993). Peta geologi lembar Baturaja, Sumatera. Pusat Penelitian dan Pengembangan Geologi.

Ghose, R., Yoshioka, S., & Oike, K. (1990). Three-dimensional numerical simulation of the subduction dynamics in the Sunda arc region, Southeast Asia. Tectonophysics, 181(1–4), 223–255. https://doi.org/10.1016/0040-1951(90)90018-4

Halauwet, Y., Afnimar, Triyoso, W., Vackář, J., Daryono, D., Supendi, P., Daniarsyad, G., Simanjuntak, A. V. H., Pranata, B., Narwadan, H. A. A. M., & Hakim, M. L. (2024). A new automated procedure to obtain reliable moment tensor solutions of small to moderate earthquakes ($3.0 \leq M \leq 5.5$) in the Bayesian framework. Geophysical Journal International, 239(2), 1000–1020. https://doi.org/10.1093/gji/ggae309

Hall, R., Clements, B., Smyth, H. R., & Cottam, M. A. (2007). A new interpretation of Java's structures. Proceedings Indonesian Petroleum Association, May, IPA07-G-035.

Hamilton, W. B. (1988). Plate tectonics and island arcs. Special Paper of the Geological Society of America, 100, 1503–1527. https://doi.org/10.1130/SPE253-p113

Haryanto, I. (1999). Tektonik Sesar Baribis daerah Majalengka Jawa Barat. Institut Teknologi Bandung.

Haryanto, I., Hutabarat, J., Sudradjat, A., Ilmi, N. N., & Sunardi, E., 2017, Tektonik Sesar Cimandiri, Provinsi Jawa Barat. In Bulletin of Scientific Contribution (pp. 255–274). http://jurnal.unpad.ac.id/bsc/article/view/15103.

Hidayat, E., 2010, Analisis morfotektonik Sesar Lembang, Jawa Barat. Widyariset, 13(2), 83–92. https://doi.org/10.14203/widyariset.13.2.2010.83-92.

Huchon, P. & Le Pichon, X., 1984, Sunda Strait and Central Sumatra Fault. Geology, 12(11), 668–672. https://doi.org/10.1130/0091-7613(1984)12<668:SSACSF>2.0.CO;2.

Hussain, E., Gunawan, E., Hanifa, N.R. & Zahro, Q., 2023, The seismic hazard from the Lembang Fault, Indonesia, derived from InSAR and GNSS data. Natural Hazards and Earth System Sciences, 23(10), 3185–3197. https://doi.org/10.5194/nhess-23-3185-2023.

Irsyam, M., Widiyantoro, S., Natawidjaja, D.H., Meilano, I., Ariska, R., Hidayati, S., Triyoso, W., Rahma, H., Didiek, D., Lutfi, F. & Sunarjito., 2017, Peta sumber dan bahaya gempa Indonesia tahun 2017 (1st ed.). Pusat Penelitian dan Pengembangan Perumahan dan Permukiman, Kementerian Pekerjaan Umum dan Perumahan Rakyat, Badan Penelitian dan Pengembangan, Kementerian Pekerjaan Umum dan Perumahan Rakyat.

Koesmono, M., Kusnama & Suwarna, N., 1996, Peta geologi lembar Sindabarang dan Bandarwaru, Jawa. Pusat Penelitian dan Pengembangan Geologi.

Logue, A.S., 2015, Orientation of the maximum horizontal stress (SHmax) in the Orange basin and Outeniqua sub-basins of South Africa : neotectonic implications. University of Cape Town. http://hdl.handle.net/11427/19995.

Lund, B. & Townend, J., 2007, Calculating horizontal stress orientations with full or partial knowledge of the tectonic stress tensor. Geophysical Journal International, 170(3), 1328–1335. https://doi.org/10.1111/j.1365-246X.2007.03468.x.

Malod, J. A., Karta, K., Beslier, M. O. & Zen, M. T., 1995, From normal to oblique subduction: Tectonic relationships between Java and Sumatra. Journal of Southeast Asian Earth Sciences, 12(1–2), 85–93. https://doi.org/10.1016/0743-9547(95)00023-2.

Mangga, S.A., Amirudin, Suwarti, S. & Gafoer, S., 1993, Peta geologi lembar Tanjungkarang, Sumatera.

Marliyani, G.I., Arrowsmith, J.R., & Whipple, K.X., 2016, Characterization of slow slip rate faults in humid areas: Cimandiri Fault Zone, Indonesia. Journal of Geophysical Research: Earth Surface, 121(12), 2287–2308. https://doi.org/10.1002/2016JF003846.

Marliyani, G.I., Helmi, H., Arrowsmith, J.R. & Clarke, A., 2020, Volcano morphology as an indicator of stress orientation in the Java Volcanic Arc, Indonesia. Journal of Volcanology and Geothermal Research, 400, 106912. https://doi.org/https://doi.org/10.1016/j.jvolgeores.2020.106912.

Meilano, I., Abidin, H.Z., Andreas, H., Gumilar, I., Sarsito, D., Rahma, H., Rino, Harjono, H., Kato, T., Kimata, F. & Fukuda, Y., 2012, Slip rate estimation of the Lembang Fault West Java from geodetic observation. Journal of Disaster Research, 7(1), 12–18. https://doi.org/10.20965/jdr.2012.p0012.

Mohamed, M., Orr, D., Meguid, A., Crane, B. & Squires, S., 2016, Multistage horizontal hydraulic fracture optimization through an integrated design and workflow in Apollonia tight chalk, Egypt from the laboratory to the field. https://doi.org/10.2118/183068-MS.

P.H. Silitonga, 1973, Peta geologi lembar Bandung, Jawa. Pusat Penelitian dan Pengembangan Geologi.

Pramumijoyo, S. & Sebrier, M., 1991, Neogene and quaternary fault kinematics around the Sunda Strait area, Indonesia. Journal of Southeast Asian Earth Sciences, 6(2), 137–145. https://doi.org/10.1016/0743-9547(91)90106-8.

Pratama, W.N. & Kita, S., 2022, Stress field orientation obtained from earthquake focal mechanisms in Indonesia region.

Pulunggono, A. & Martodjojo, S., 1994, Perubahan tektonik Paleogen-Neogen merupakan peristiwa tektonik tertpenting di Jawa. Proccedings Geologi

Dan Geotektonik Pulau Jawa, 37–50.

Purnomo, H. & Tobing, E.M., 2007, Pengembangan simulator pengendalian sumur pada pemboran vertikal, berarah, maupun horizontal. Lembaran Publikasi Minyak dan Gas Bumi, 41(1), 11. https://doi.org/https://doi.org/10.29017/LPMGB.41.1.48.

Ramdhan, A.M., 2021, In situ stress and stress regime in the onshore part of the Northeast Java Basin. Scientific Contributions Oil and Gas, 44(2), 13. https://doi.org/https://doi.org/10.29017/SCOG.44.2.591.

Ranneft, T.S.M., 1979, Segmentation of island arcs and application to petroleum geology. Journal of Petroleum Geology, 1(3), 35–53. https://doi.org/10.1111/j.1747-5457.1979.tb00618.x.

Rostami, E., Boness, N. & Zoback, M., 2020, Significance of well orientation on cumulative production from wells in the Bakken Region. https://doi.org/10.15530/urtec-2020-2813.

Rusmana, E., Suwitodirdjo, K., Suwitoditdjo, K. & Suharsono., 1991, Peta geologi lembar Serang, Jawa. Pusat Penelitian dan Pengembangan Geologi.

Santosa., 1991, Peta geologi lembar Anyer, Jawa Barat. Pusat Penelitian dan Pengembangan Geologi.

Shamim, S., Khan, P.K. & Mohanty, S.P., 2019, Stress reconstruction and lithosphere dynamics along the Sumatra subduction margin. Journal of Asian Earth Sciences, 170, 174–187. https://doi.org/10.1016/j.jseaes.2018.11.008.

Sieh, K. & Natawidjaja, D., 2000, Neotectonics of the Sumatran Fault, Indonesia. Journal of Geophysical Research, 105(No. B12), 28,295-28326.

Sudjatmiko, 1972, Peta geologi lembar Cianjur, Jawa. Pusat Penelitian dan Pengembangan Geologi.

Sukamto, 1975, Peta geologi lembar Jampang dan Balekambang. Peta geologi lembar Jampang dan Balekambang.

Supendi, P., Nugraha, A.D., Puspito, N.T., Widiyantoro, S. & Daryono, D., 2018, Identification of active faults in West Java, Indonesia, based on earthquake hypocenter determination, relocation, and focal mechanism analysis. Geoscience Letters, 5(1). https://doi.org/10.1186/s40562-018-0130-y.

Supendi, P., Widiyantoro, S., Rawlinson, N., Yatimantoro, T., Muhari, A., Hanifa, N.R., Gunawan, E., Shiddiqi, H. A., Imran, I., Anugrah, S.D., Daryono, D., Prayitno, B.S., Adi, S.P., Karnawati, D., Faizal, L. & Damanik, R., 2023, On the potential for megathrust earthquakes and tsunamis off the southern coast of West Java and southeast Sumatra, Indonesia. Natural Hazards, 116(1), 1315–1328. https://doi.org/10.1007/S11069-022-05696-Y/FIGURES/6.

Susilohadi, 2019, Atlas seismik refleksi dangkal Selat Sunda Timur Laut dan Teluk Lampung (L. Arifin, M. Hanafi, D. Kusnida, & R. Rahardiawan (eds.); 1st ed.). Pusat Penelitian dan Pengembangan Geologi Kelautan.

Susilohadi, S., Gaedicke, C. & Djajadihardja, Y., 2009, Structures and sedimentary deposition in the Sunda Strait, Indonesia. Tectonophysics, 467, 55–71. https://doi.org/10.1016/j.tecto.2008.12.015

Tingay, M., Morley, C., King, R., Hillis, R., Coblentz, D. & Hall, R., 2012, Present-day stress field of Southeast Asia. Tectonophysics, 482(1–4), 92–104. https://doi.org/10.1016/j.tecto.2009.06.019.

Tjia, 1968, The Lembang Fault. Geologie En Minjnbouw, 47 (2), 126–130.

Tjia, H.D., 2001, Wrench tectonics in Sundaland - subsurface and offshore evidence. Geological Society of Malaysia Annual Geological Conference, 71–77.

Tunggal, T., 2000, Horizontal well performance modelling using pseudowell technique. Scientific Contributions Oil and Gas, 23(2), 7. https://doi.org/https://doi.org/10.29017/SCOG.23.2.1081.

Turkandi, T., Sidarto, Agustiyanto, D.A. & Hadiwidjoyo, M.M.P., 1992, Peta geologi lembar Jakarta dan Kepulauan Seribu, Jawa. Pusat Penelitian dan Pengembangan Geologi.

Van Bemmelen, R.W., 1949, The geology of Indonesia. general geology of Indonesia and adjacent archipelagoes. In Government Printing Office, The Hague (pp. 545-547; 561-562). https://doi.org/10.1109/VR.2018.8447558.

Van Bemmelen, R.W., 1970, The geology of Indonesia (second edition). The Hague, Goverment Printing Office.

Widarsono, B., 2000, In-situ stresses in rock masses: A general review. Scientific Contributions Oil and Gas, 23(2), 14. https://doi.org/https://doi.org/10.29017/SCOG.23.2.881.

Widiyantoro, S., Supendi, P., Ardianto, A., Baskara, A.W., Bacon, C.A., Damanik, R., Rawlinson, N., Gunawan, E., Sahara, D.P., Zulfakriza, Z., Husni, Y. M. & Lesmana, A., 2022, Implications for fault locking south of Jakarta from an investigation of seismic activity along the Baribis Fault, northwestern Java, Indonesia. Scientific Reports, 12(1), 6–15. https://doi.org/10.1038/s41598-022-13896-6.

Yang, F., 2014, Performance comparison of transverse and longitudinal fractured horizontal wells over varied reservoir permeability [Missouri University of Science and Technology]. https://scholarsmine.mst.edu/masters_theses/7348/.

Yulianto, I., Hall, R., Clements, B. & Elders, C.R., 2007, Structural and stratigraphic evolution of the offshore Malingping Block, West Java, Indonesia. Proceedings Indonesian Petroleum Associatiion Thirty-First Annual Convention Annual Convention, May. https://doi.org/10.29118/ipa.2540.07.g.036.

Zen, M.T. & Sudrajat, A., 1983, History of the Krakatau volcanic complex in strait and the mitigation of its future hazards. In Buletin Jurusan Geologi (pp. 1–28). Institut Teknologi Bandung.

Zoback, M.L., 1992, First-and second-order patterns of stress in the lithosphere: the world stress map project. Journal of Geophysical Research, 97(B8), 11,703-11,728. https://doi.org/10.1029/92jb00132.